

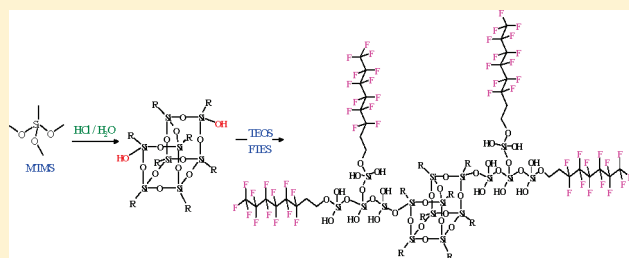
# Phase Segregation of Polymethylsilsesquioxane in Antireflection Coatings

Wen-Pin Chuang,<sup>†,‡</sup> Yuung-Ching Sheen,<sup>†</sup> Su-Mei Wei,<sup>†</sup> Chih-Chun Teng,<sup>‡</sup> Ming-Yu Yen,<sup>‡</sup> and Chen-Chi M. Ma<sup>\*,‡</sup>

<sup>†</sup>Division of Applied Chemistry, Material and Chemical Research Laboratories, Industrial Technology Research Institute, Hsinchu, Taiwan

<sup>‡</sup>Department of Chemical Engineering, National Tsing Hua University, Hsinchu, Taiwan

**ABSTRACT:** We herein describe the preparation and characterization of a phase-separated fluorinated polymethylsilsesquioxane (PMSQ), which may be used as an antireflective coating. The results of FTIR analysis showed that when PMSQ is synthesized from methyltrimethoxysilane (MTMS), it exists mostly in the form of a cage structure. Its reflectivity of normally incident light ( $R$ ) may be reduced from 3.9 to 0.9% by grafting 1H,1H,2H,2H-perfluorooctyltriethoxysilane (FTES) by means of a sol–gel process. In the study described herein, the minimum reflectivity of PMSQ was lowered to less than 1% by coating it with a single layer of fluorinated polymethylsilsesquioxane, through phase segregation of PMSQ and FTES that took place during film formation. The RI of PMSQ at 550 nm was also reduced from 1.51 to 1.42 by heating at 80 °C for 30 min, a temperature suitable for substrates, such as plastics, that have low heat resistance. Wetting and adhesion to substrates were both improved by the additional grafting of tetraethoxysilane (TEOS), again by means of a sol–gel process. Results of solid-state  $^{29}\text{Si}$  NMR and GPC showed increases in  $T_3$ ,  $Q_3$ ,  $Q_4$ , and the molecular weight, which signal the effective grafting of both the TEOS and the FTES on the PMSQ. Results from energy-dispersive X-ray spectroscopy (EDX) show that the quantity of fluorine atoms at the surface of the PMSQ film increased from 0 to 22%, providing the evidence of the phase segregation within the PMSQ film. When FTES is used, we found an increase in the water contact angle from 92° to 108°, which indicated that the hydrophobicity at the PMSQ film surface increased by increasing the FTES content from 0 to 100 wt %, using the weight of MTMS as 100%.



## 1. INTRODUCTION

Antireflection (AR) coatings are used to maximize the transmission of light through optical surfaces and to achieve the desired levels of contrast and brightness in such devices as plasma display panels (PDPs) and liquid crystal displays (LCDs). They are widely applied to solar cells, lasers, and other photovoltaic devices as well as to all types of optical lenses.<sup>1–5</sup> AR is achieved through the destructive interference that occurs between the light reflected from the air–coating and coating–substrate interfaces.<sup>6</sup>

The substrate that is most commonly used for optical applications is crown glass, which has a refractive index (RI) of about 1.52. The materials most commonly used for AR coatings are magnesium fluoride<sup>24</sup>  $\text{MgF}_2$  (RI = 1.38) and fluoropolymers (some of which have an RI as low as 1.30,<sup>28</sup> but fluoropolymers with such a low RI are more difficult to apply due to their poor wetting and adhesion to substrates). By coating crown glass with  $\text{MgF}_2$ , its reflectivity may be reduced from 4 to 1.5%.  $\text{MgF}_2$  is commonly used as a coating because of its low cost and adaptability to wavelengths in the middle of the visible band, thereby enabling a reasonably high level of antireflection.<sup>15</sup> However, a single layer coating cannot reduce the reflectivity below 1%. By using multilayer coatings that consist of a material with a lower RI (e.g., silica; RI = 1.5) together with a material with a higher RI (e.g.,  $\text{TiO}_2$ ; RI = 2.3), a reflectivity as low as 0.1% may be obtained for a single wavelength.<sup>23</sup> Multilayer coatings that afford very low reflectivity over a broad band may also

be made, although these are difficult to manufacture and relatively expensive.<sup>17,23</sup>

As an alternative to the use of destructive interference, nanoporous structures may also be used for antireflective coatings.<sup>7–10</sup> A number of techniques have been proposed for the fabrication of porous polymer films.<sup>7–10</sup> In the range of visible light, the transmittance of a microphase-separated film formed by the removal of a single component can be as high as 99.5%.<sup>7,8</sup> A nanoporous multilayer film processed using the breath-figure method, and having a gradually varying porosity ratio, was shown to provide low reflection ( $R = 0.74\%$ ) in the near-IR range (900–2200 nm).<sup>9</sup> Polyelectrolytes and charged colloidal particles assembled using layer-by-layer (LBL) technique demonstrated excellent AR in the visible ranges ( $R = 0.14\%$ ).<sup>10</sup> However, although nanoporous structures may be used to achieve a low reflectivity over a broad band, the costs are high due to the complexity of the method of fabrication of nanoporous structures.

In comparison with nanoporous structures, the destructive interference method has great practical value and widely used for AR coatings because destructive interference has advantages of scale associated with the fabrication of large surface areas and

Received: March 29, 2011

Revised: May 27, 2011

Published: June 06, 2011

the phenomenon are less expensive to produce. Some fluoropolymers, such as fluoroacrylates, are commercially available as AR coatings, although a primer,<sup>29</sup> such as acrylate resin, is necessary to improve wetting and adhesion to the substrate. The reflectivity may be lowered to 1% or less by using the double-layer coating of the primer and fluoropolymer layers.<sup>29</sup>

The aim of our study was to prepare a polymethylsilsequioxane (PMSQ) grafted with FTES and TEOS, which has a low reflectivity and RI, together with the appropriate properties of wettability and adhesion. The hydrophilic parts of PMSQ (such as the hydroxyl groups) attach to the glass substrate via hydrogen bonding. The hydrophobic parts (such as the fluoro groups) can migrate to the film surface and form phase-segregated structures that cause the desired low reflectivity (less than 1%). Furthermore, the PMSQ film described herein may be formed at 80 °C, a temperature that may be applied safely to substances that have a low heat resistance, such as plastics.

## 2. EXPERIMENTAL SECTION

**2.1. Materials.** The materials used in the experiments were methyltrimethoxysilane (MTMS, 98%; Aldrich), tetrahydrofuran (THF, 99%, stabilized and anhydrous; Acros), methyl *n*-propyl ketone (MPK, 99%; Acros), hydrochloric acid (35%; Yakuri), tetraethoxysilane (TEOS, 99%; Acros), and 1H,1H,2H,2H-perfluorooctyltriethoxysilane (FTES, 98%; Aldrich).

**2.2. Preparation of Polymethylsilsequioxane (PMSQ).** The formulation and synthesis of the PMSQ are shown in Scheme 1. PMSQ was synthesized first, and different amounts of TEOS and FTES were then grafted to it. We now describe the procedure, using a weight ratio of MTMS:TEOS:FTES of 1:0.5:0.25 as an example. In this case, synthesis of the PMSQ was achieved by placing 34 g (42 mL) MPK and 15 g (16 mL) MTMS in a 200 mL, four-necked flask and cooling it for 10 min in an ice bath. 3 g of deionized water, together with 0.05 g of hydrochloric acid dissolved in 19 g (21 mL) of THF, were then added to the flask dropwise over a period of 30 min, accompanied by vigorous magnetic stirring. The reaction flask was then warmed to room temperature, and the stirring was continued for 30 min at room temperature. Hydrolysis and condensation were achieved by maintaining the flask at 60 °C for 3 h in an oil bath under nitrogen under reflux conditions. The grafting of the TEOS on the PMSQ was then achieved by dissolving 7.5 g (8 mL) of TEOS dissolved in 10 g (12 mL) of MPK in the solution and allowing reaction for 2 h at 60 °C. Similarly, the grafting of the FTES was also achieved by adding 3.75 g (3 mL) of FTES dissolved in 5 g (6 mL) of MPK to the solution, heating for a further 2 h at 60 °C.

Using the methods described above, the PMSQ precursor solution was synthesized, enabling its structural characterization. Summarized details of its formulation are presented in Table 1. The parameters of the weight ratio of MTMS to TEOS and FTES to TEOS were varied in order to study the effects of this variation on the molecular structures, the molecular weight, the RI, and the reflectivity of the PMSQ. The weight ratio of MTMS to TEOS was set at 2.0, 3.0, and 4.0:1. The weight ratio of FTES to TEOS was adjusted to 0.5, 1.0, 1.5, and 2.0 for a fixed weight ratio of MTMS to TEOS.

**2.3. Preparation of Powder and Films for Analysis.** The untreated PMSQ (the "precursor") was passed through a 0.25  $\mu$ m filter and then dried in a vacuum at 80 °C for 4 h. The dried cake was ground to a powder for use in solid-state <sup>29</sup>Si NMR analyses. In order to prepare a set of PMSQ thin films, the precursor (20 wt % PMSQ in MPK) was filtrated with a 0.25  $\mu$ m filter and spin-coated at 1500 rpm for 30 s on silicon wafers or glass substrates at room temperature (PM490, Swien Co., Taiwan). The film was then maintained at a temperature of 80 °C on a hot plate for 30 min, so that the solvent could be removed.

**2.4. Structural Characterization.** Nuclear magnetic resonance (NMR) spectroscopy was used to investigate the structure of the materials at a molecular level and to provide data on the degree of condensation in the polymer network. Solid-state <sup>29</sup>Si NMR spectra were obtained using a spectrometer (Bruker DSX400WB) at 79.37 MHz. The resulting spectra were deconvoluted using a Lorentz–Gaussian fit. The Fourier transform infrared (FT-IR) spectra of the PMSQ were recorded between 400 and 4000 cm<sup>-1</sup> using a Nicolet Avatar 320 FT-IR spectrometer (Nicolet Instrument Corp., Madison, WI). The PMSQ sample was coated on a KBr plate. The average of a minimum of 32 scans was obtained, using a resolution of 2 cm<sup>-1</sup> within the range 400–4000 cm<sup>-1</sup>. The characteristic absorption peaks of the functional group were thus identified. Using THF as the solvent, a Waters 510 GPC (RI detector) was used to determine the molecular weights of the PMSQ (at a flow rate of 1 mL/min). The GPC calibration curves were obtained using polystyrene standards.

**2.5. Optical Property Analyses.** The RIs of the PMSQ films were recorded using a variable-angle spectroscopic ellipsometer (VESA, J.A. Woollam Co.) equipped with a He–Ne laser, using an angle of incidence in the range 70°–80°. The measurement of reflectivity of normally incident light was achieved for the PMSQ film using a Shimadzu 3600 UV/vis/near-IR spectrometer with an integrating sphere. The spectra were recorded automatically at 2 nm intervals of incident light for wavelengths between 240 and 2600 nm. The RI and reflectivity data presented are the average and standard deviation of at least five measurements made at different areas on the film surface.

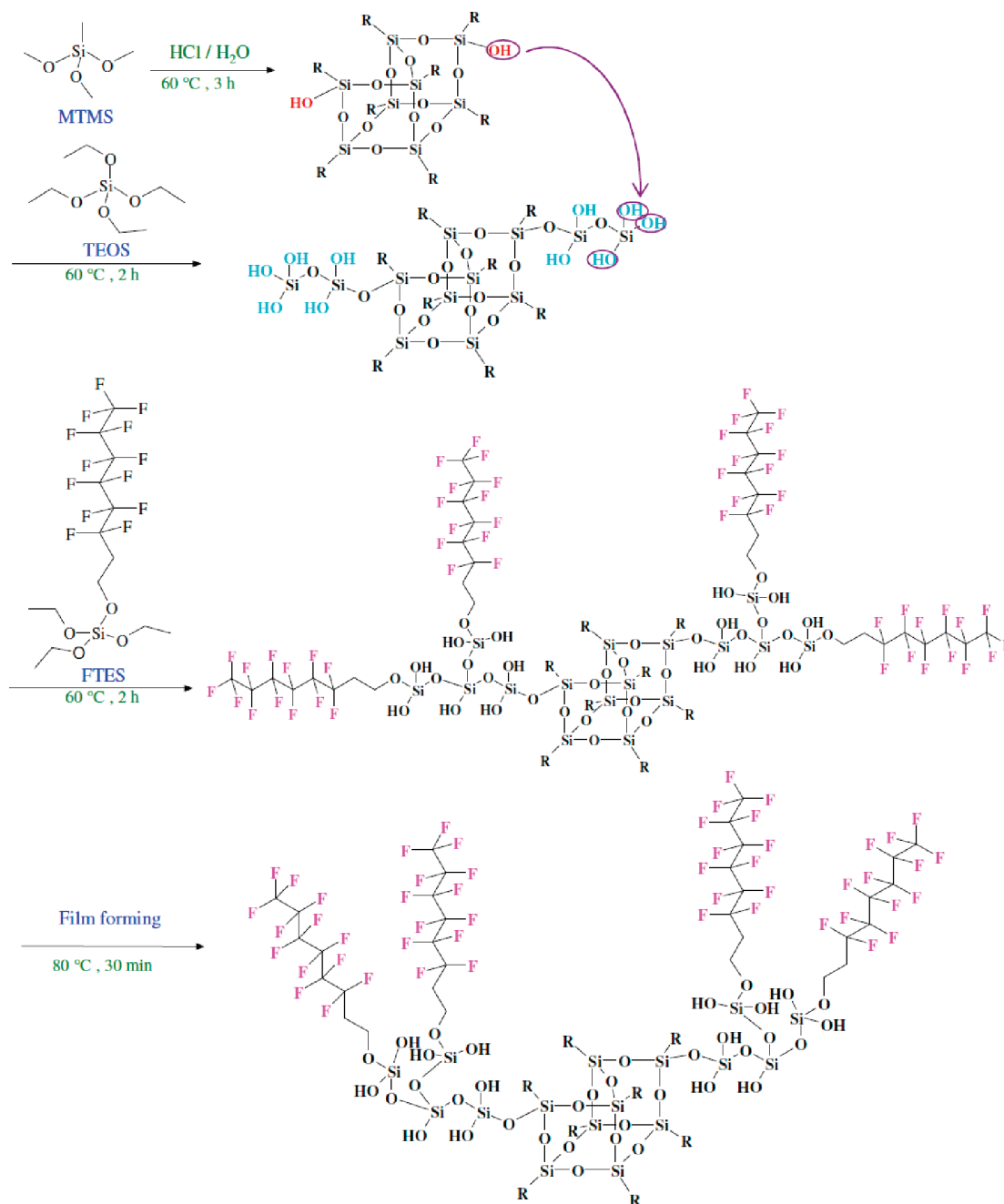
**2.6. Analyses of Surface Properties.** Scanning electron microscopy (SEM) analyses were performed using a JSM-5600 (Japan) model scanning electron microscope with an attached light element detector. The electron beam energy was 15 keV. Data were collected from a scanned region using a live capture time of 130 s, and commercially available software (Link ZAF-4, Oxford Instruments) was used to calculate the atomic number in each case. The static contact angle of deionized water drops on the surface of the PMSQ films was measured within a period of 10 s at room temperature by means of a face-contact angle meter (Kyowa Interface Science, CA-D Type). The advancing and receding angles of contact of water on the PMSQ films coated on the glass substrates were measured by means of a contact angle meter. The water contact angle data presented are the average and standard deviation of at least five measurements made at different areas on the film surface.

## 3. RESULTS AND DISCUSSION

**3.1. Preparation and Characterization of the PMSQ.** In the present study, FTES was grafted to PMSQ in order to reduce its reflectivity and RI at low temperatures, in preference to the incorporation of porosity by means of baking at high temperature. However, the low surface energy of the FTES reduced the effectiveness of the wetting and adhesion on the substrates. TEOS was therefore used to promote wetting and adhesion. As shown in Scheme 1, the grafting of a single molecule of TEOS on PMSQ causes an increase in the number of hydroxyl groups at the end from one to three. Hence, wetting and adhesion on the substrates may be greatly improved and a greater amount of FTES may be grafted, as a result of the increased number of hydroxyl groups.

The structural identification was confirmed by FTIR and NMR. Figure 1 shows the FTIR spectra of the PMSQ film. The Si–O–Si backbone is represented by a broad band of absorption in the range of wave numbers of 1000–1250 cm<sup>-1</sup>. The Si–CH<sub>3</sub> absorption bands may be seen at 1273 and 768 cm<sup>-1</sup>. The corresponding CH<sub>3</sub> absorption band appears at around 2973 and 2844 cm<sup>-1</sup>. The absorption band at 3200–3600 cm<sup>-1</sup>, which corresponds to the hydroxyl functional group, was obtained

Scheme 1. Preparation of Polymethylsilsesquioxane AR Coating



following the hydrolysis of MTMS. The corresponding Si—OH absorption band appears at  $910\text{ cm}^{-1}$ . An interesting characteristic of the FTIR spectra of PMSQ has been reported<sup>11–16</sup> in the splitting of the Si—O—Si absorption into two bands at around  $1130$  and  $1070\text{ cm}^{-1}$ , which correspond to the regular/cage and irregular/random network, respectively. The Si—O—Si absorption band of pure PMSQ may be seen at around  $1120\text{ cm}^{-1}$ , and the hydroxyl group was still present after condensation, which shows that the synthesized PMSQ exists in a partial cage structure.<sup>18,27</sup> The C—F absorption peak appeared at  $1240\text{ cm}^{-1}$  after grafting with FTES.<sup>26</sup> The random network structures began to appear at  $1070\text{ cm}^{-1}$  after grafting with 50 wt % TEOS, taking the weight of MTMS as 100%, and the degree of the random network structure

increased with increasing FTES content, which indicates that the main structure of the PMSQ was changed by the addition of TEOS and FTES.

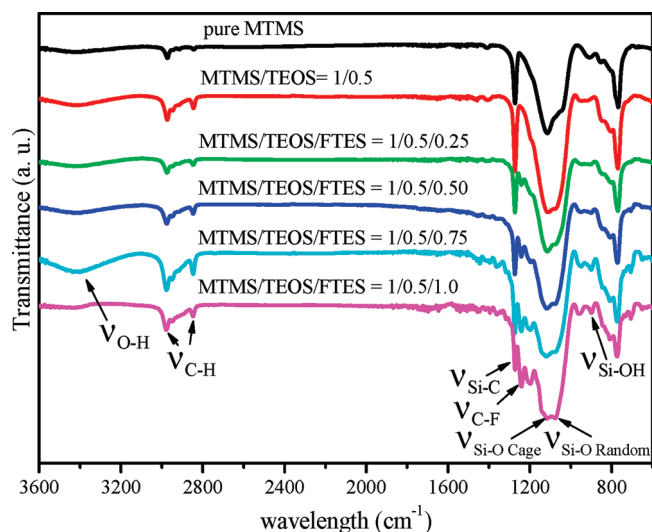
The solid-state  $^{29}\text{Si}$  NMR spectra of the synthesized PMSQ are shown in Figure 2. A summary of the results is presented in Table 2. The hydrolysis and condensation reaction of MTMS are shown in Figure 2a. The chemical shifts of the PMSQ with two (T2) and three (T3) siloxane bonds (Si—O—Si) may be observed at  $-57$  and  $-65\text{ ppm}$ , respectively.<sup>19–22</sup> The chemical shift of the MTMS monomer at  $-37$  to  $-41\text{ ppm}$  is not seen in Figure 2a. These results point to the completion of the hydrolysis and condensation reactions of the MTMS. The larger peak (T3) of the PMSQ indicates the presence of the fully condensed Si



**Table 1.** Effect of Various TEOS and FTES Contents on Molecular Weight

code	weight ratio			$M_w^a$	$M_n^a$	$M_w/M_n^a$
	MTMS content	TEOS content	FTES content			
1	1	0	0	1300	800	1.6
2	1	0.25	0	1700	1000	1.7
3	1	0.25	0.125	1900	1100	1.7
4	1	0.25	0.250	2200	1300	1.7
5	1	0.25	0.375	2500	1400	1.8
6	1	0.25	0.500	2700	1500	1.8
7	1	0.33	0	1800	1100	1.6
8	1	0.33	0.165	2100	1200	1.8
9	1	0.33	0.330	2500	1400	1.8
10	1	0.33	0.495	2800	1500	1.9
11	1	0.33	0.660	3200	1700	1.9
12	1	0.50	0	2000	1200	1.7
13	1	0.50	0.250	2600	1400	1.9
14	1	0.50	0.500	3100	1600	1.9
15	1	0.50	0.750	3600	1900	1.9
16	1	0.50	1.000	4100	2100	2.0

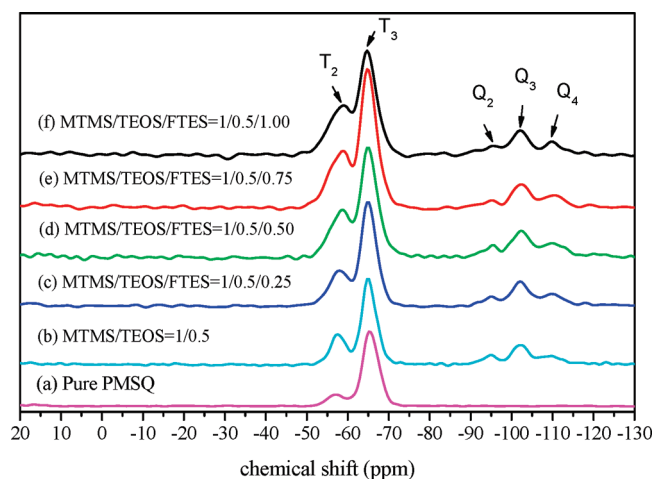
<sup>a</sup> Determined by GPC using polystyrene as standards and THF as solvent.

**Figure 1.** FTIR spectra of PMSQ grafted with TEOS and FTES.

atom of the  $\text{SiO}_{1.5}$  unit in the defective branching structures. The smaller peak (T2) is caused by the defective Si atom that is connected to the hydroxyl group. The characterization obtained from the results of the solid-state  $^{29}\text{Si}$  NMR reveal that the synthesized cage structure of PMSQ possesses some defective branching structures.

Figure 2b shows that after the TEOS was grafted to the PMSQ three smaller peaks emerged at  $-95$ ,  $-101$ , and  $-110$  ppm, which could respectively be attributed to the chemical shifts of two ( $\text{Q}_2$ ), three ( $\text{Q}_3$ ), and four ( $\text{Q}_4$ ) siloxane bonds ( $\text{Si}-\text{O}-\text{Si}$ ). Figures 2c–f show that on further grafting of the PMSQ with different amounts of FTES the magnitudes of the T2 and  $\text{Q}_2$  peaks reduce and those of the T3,  $\text{Q}_3$ , and  $\text{Q}_4$  increase with increasing FTES content, giving further clear evidence of the successful grafting of TEOS and FTES to the PMSQ.

The results of the GPC analyses of PMSQ grafted with different amounts of TEOS and FTES are summarized in Table 1.

**Figure 2.** Solid-state  $^{29}\text{Si}$  NMR spectra of PMSQ.

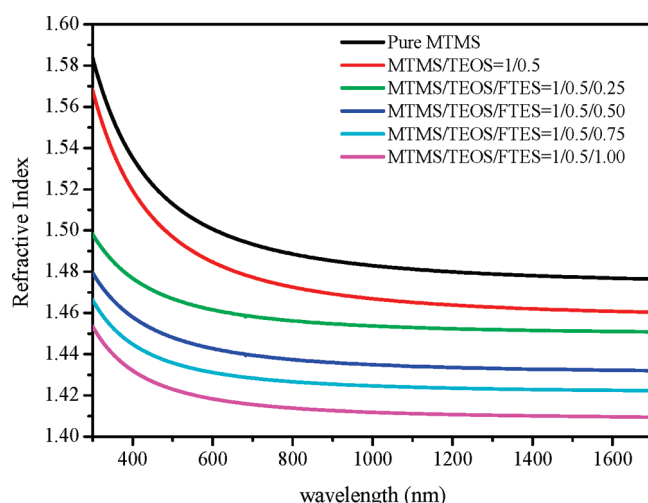
As previously reported,<sup>11</sup> the molecular weight of PMSQ was controlled by the molar ratios of water to monomer ( $\text{R}_1$ ) or catalyst to monomer ( $\text{R}_2$ ). Both the molecular weight and the polydispersity index (PDI) increased with increasing  $\text{R}_1$  and  $\text{R}_2$ , although the molecular structures and stability of PMSQ were difficult to control when  $\text{R}_1$  and  $\text{R}_2$  were increased. In the present study, the molecular weight was controlled by varying the TEOS and FTES content, which both makes it easy to control the molecular structures and lends a degree of stability to the resulting structure. The relative average molecular weight of the PMSQ synthesized using MTMS was 1300 (calibrated with PS standards), and the PDI was 1.6. When the weight ratio of MTMS:TEOS:FTES was 1:0.5:1, the relative molecular weight increased to 4100 (calibrated with PS standards) and the PDI was maintained at 2.0, which demonstrates that the molecular structure was under control. Both the molecular weight and the PDI increase after grafting with TEOS and FTES, providing further evidence of the successful grafting of TEOS and FTES on the PMSQ.

**3.2. Optical Properties.** The variation in RI of the PMSQ is shown in Figure 3, and the effects of grafting different amounts of TEOS and FTES on the PMSQ are summarized in Table 3. The RI of pure PMSQ is around 1.5 at 550 nm. As reported elsewhere,<sup>8,9</sup> the RI cannot be reduced to 1.42 or lower without heating to at least  $400^\circ\text{C}$  to allow the incorporation of pores in the matrix of the polymer. The introduction of FTES into PMSQ causes the RI to be lowered even after heating at  $80^\circ\text{C}$ , which makes the material suitable for substrates, such as plastics, that have a low heat resistance. The RI decreased slightly when grafted with TEOS ( $\text{RI} = 1.46$ ) and decreased significantly on further grafting with FTES (yielding an RI of 1.35). The grafting of increasing quantities of TEOS and FTES to the PMSQ led to ever lower RI values. When the weight ratio of MTMS:TEOS:FTES was 1:0.5:1 (labeled as code 16 in Table 3), the RI at 550 nm was 1.42, which was even lower than the theoretical value of 1.44. This result could have been caused by the molecular arrangement of the PMSQ that was grafted with FTES, which is not as compact as pure PMSQ. For any material, the RI increases with the density of the molecular structure. The original structure of the PMSQ was regular, allowing for more compact arrangement of the molecules, and leading to a higher RI. After grafting with TEOS and FTES, the PMSQ random network

**Table 2.** Results of Solid-State  $^{29}\text{Si}$  NMR and Water-Contact Angle of PMSQ Grafted with TEOS and FTES

weight ratio			solid-state $^{29}\text{Si}$ NMR siloxane units (%)					water contact angle (deg)	
MTMS	TEOS	FTES	T <sub>2</sub>	T <sub>3</sub>	Q <sub>2</sub>	Q <sub>3</sub>	Q <sub>4</sub>	advancing angle <sup>a</sup>	contact angle hysteresis <sup>b</sup>
1	0	0	14	86	0	0	0	100 ± 0.7	14 ± 0.2
1	0.5	0	32	68	25	48	27	98 ± 1.0	15 ± 0.5
1	0.5	0.25	31	69	22	50	28	105 ± 1.6	12 ± 0.8
1	0.5	0.5	30	70	21	50	29	105 ± 1.1	12 ± 0.6
1	0.5	0.75	27	73	20	51	29	106 ± 1.3	11 ± 0.7
1	0.5	1.0	26	74	18	52	30	106 ± 1.5	9 ± 0.7

<sup>a</sup> Determined by static contact angle meter. <sup>b</sup> The difference between advancing and receding contact angles.

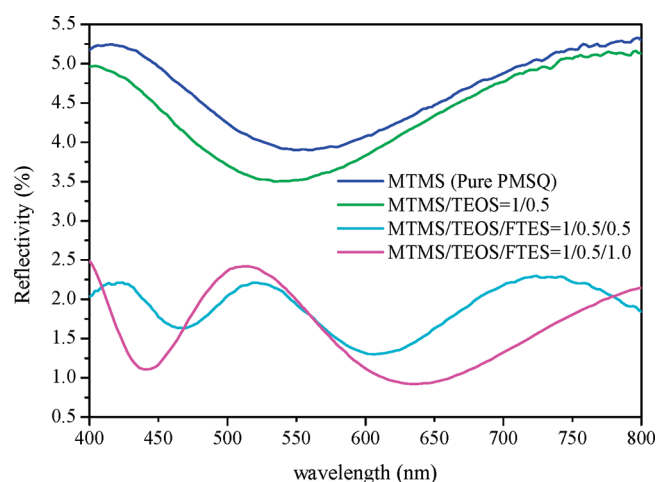
**Figure 3.** Refractive indices of PMSQ grafted with TEOS and FTES.**Table 3.** Optical Properties and Surface Analyses of PMSQ grafted with Different Amounts of TEOS and FTES

code	RI <sup>a</sup>	minimum reflectivity (%) <sup>b</sup>	fluorine atom (%) <sup>c</sup>	silicon atom (%) <sup>c</sup>	water contact angle (deg) <sup>d</sup>
1	1.51 ± 0.008	3.9 ± 0.06	0	32	93 ± 0.8
2	1.50 ± 0.006	3.7 ± 0.04	0	33	93 ± 0.2
3	1.48 ± 0.004	2.0 ± 0.03	5	24	99 ± 1.3
4	1.47 ± 0.005	1.7 ± 0.02	10	18	103 ± 1.1
5	1.46 ± 0.006	1.5 ± 0.01	11	13	104 ± 1.4
6	1.45 ± 0.005	1.4 ± 0.01	14	8	106 ± 1.3
7	1.50 ± 0.007	3.6 ± 0.05	0	33	92 ± 0.6
8	1.47 ± 0.004	1.8 ± 0.03	7	25	98 ± 1.0
9	1.46 ± 0.005	1.5 ± 0.02	11	20	103 ± 0.8
10	1.45 ± 0.003	1.3 ± 0.01	16	12	105 ± 1.1
11	1.44 ± 0.002	1.2 ± 0.01	19	6	107 ± 1.6
12	1.49 ± 0.005	3.5 ± 0.07	0	36	91 ± 0.6
13	1.46 ± 0.004	1.6 ± 0.05	8	28	97 ± 0.7
14	1.45 ± 0.005	1.3 ± 0.03	14	18	101 ± 0.7
15	1.43 ± 0.003	1.1 ± 0.01	18	7	104 ± 0.8
16	1.42 ± 0.002	0.9 ± 0.01	22	3	108 ± 1.8

<sup>a</sup> Refractive index at 550 nm. <sup>b</sup> The minimum reflectivity between visible light (400–800 nm). <sup>c</sup> Determined by EDX. <sup>d</sup> Determined by static contact angle meter.

structure showed an apparent increase, as seen in the FTIR results. The irregular structure caused the molecular structure to be more widely spaced significantly. The RI may therefore be lower than the theoretical value.

The relationship between reflectivity and RI may be expressed by eq 1.  $R$  is the minimum reflectivity for a single layer of coating,

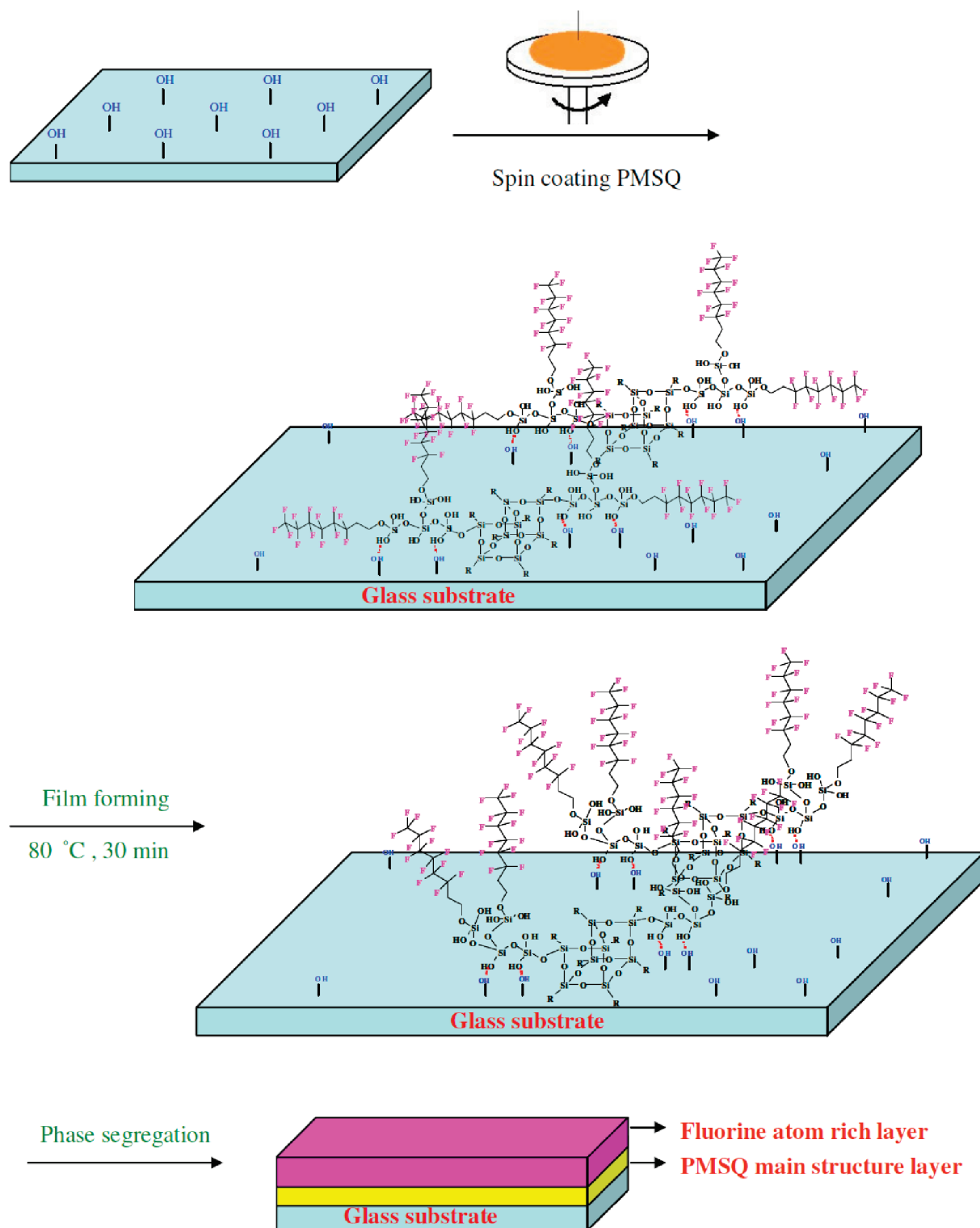
**Figure 4.** Reflectivity of PMSQ grafted with TEOS and FTES.

and  $n_s$ ,  $n_a$ , and  $n_c$  are the RIs of substrate, air, and coating, respectively. When the RI of the substrate is fixed, the lower the RI of the coating layer is and the lower the minimum reflectivity that can be reached.

$$R = \left( \frac{n_c^2 - n_a n_s}{n_c^2 + n_a n_s} \right)^2 \quad (1)$$

The reflectivity of PMSQ grafted with different amounts of TEOS and FTES is shown in Figure 4 and summarized in Table 3. The PMSQ grafted with FTES has a much lower RI than pure PMSQ; hence, the minimum reflectivity is noticeably lower. The more FTES grafted on the PMSQ, the lower the reflectivity. In comparison with pure PMSQ, the minimum reflectivity decreases from 3.9 to 0.9% when the weight ratio of MTMS:TEOS:FTES was 1:0.5:1. In common with the results for the RIs, the reflectivity was much lower than the theoretically calculated value. The minimum reflectivity calculated from eq 1 is 2.0%, which is much higher than the experimental result of 0.9%, where  $n_s$ ,  $n_a$ , and  $n_c$  are 1.52, 1.0, and 1.42, respectively. For a single layer coating, there is only one minimum value of reflectivity, such as for pure PMSQ, which has a V-shaped graph of reflectivity against wavelength. The reflectivity of PMSQ grafted with FTES (Figure 4) shows two reflectivity minima, and the graph is W-shaped, in common with that found for double-layer coatings. This finding indicates that PMSQ grafted with FTES might form a phase-segregated structure in which two separate layers occur during the formation of the film. For double-layer coatings, the minimum reflectivity may be expressed in the form of eq 2, where  $n_s$ ,  $n_a$ ,  $n_1$ ,

Scheme 2. Phase Segregation of Polymethylsilsesquioxane AR Coating



and  $n_2$  are the RIs of substrate, air, and coating layers 1 and 2, respectively.

$$R = \left( \frac{n_1^2 n_a - n_s n_2^2}{n_1^2 n_a + n_s n_2^2} \right)^2 \quad (2)$$

As illustrated in Scheme 1, PMSQ grafted with TEOS and FTES has characteristics that are both hydrophilic (such as hydroxyl groups) and hydrophobic (such as fluoro groups). The hydroxyl groups on the surface of the glass substrate become attached to those that form when the PMSQ is spin-coated on the same surface by hydrogen bonding that improves the

adhesion. The fluoro groups migrate away from the substrate toward the surface of the film during heating, and phase segregation thus takes place, as illustrated in Scheme 2. The phase segregation of the PMSQ film causes two layers to form: the first being the layer of the main structure of the PMSQ and the second being a layer rich in fluorine atoms. The ratio of fluorine atoms in this layer as measured by EDX is 22%, which is similar to that of FTES in which the corresponding ratio is 26%. The RIs of these two layers were assumed to be 1.51 and 1.35, which are respectively the RIs of pure PMSQ and pure FTES. The minimum reflectivity as calculated by eq 2 is 0.9%, which is in agreement with our experimental result.

**3.3. Surface Analyses.** Analyses such as the ratios of fluorine and silicon atoms at the surface, or the hydrophobicity of the surface, may be determined using EDX and the water contact angle. The ratios of atoms at the surface of the PMSQ grafted with different amounts of TEOS and FTES are listed in Table 3. The EDX results show that the number of silicon atoms at the surface increased when the TEOS was grafted and decreased after further grafting with FTES. However, the number of fluorine atoms at the surface increased with increasing amounts of FTES. At the surface of the PMSQ film, the quantity of silicon atoms decreased from 32 to 3%, and the quantity of fluorine atoms increased from 0 to 22%, when the weight ratio of MTMS:TEOS:FTES was 1:0.5:1, which again provides evidence of phase segregation.

The water-contact angle provides evidence of the high hydrophobicity of PMSQ due to the low surface energy of fluorine.<sup>25</sup> The water-contact angles of PMSQ grafted with different amounts of TEOS and FTES are shown in Table 3. The water-contact angle of PMSQ that contained only MTMS was 93°, and its hydrophobicity may be attributed to the methyl groups. The water-contact angle of PMSQ grafted with TEOS was slightly lower due to the increased number of hydroxyl groups. After further grafting with FTES, the water-contact angle increased dramatically to over 100°. The hydrophobicity in this case was a result of the presence of fluorine, providing further evidence of the phase segregation of the PMSQ films. The water-contact angle was 108° when the weight ratio of MTMS:TEOS:FTES was 1:0.5:1. The various water-contact angles and values of water contact angle hysteresis are listed in Table 2. A homogeneous fluorine rich surface would cause a reduction in water-contact-angle hysteresis that was related to the FTES content. The advancing water-contact angle increased from 100° to 106° and the water-contact-angle hysteresis decreased from 14° to 9° when the weight ratio of MTMS:TEOS:FTES was 1:0.5:1. The increase in the advancing water-contact angle and the decrease in the water-contact-angle hysteresis with increasing FTES content indicate that the distribution of fluorine atoms at the surface of the PMSQ film was highly uniform.

#### 4. CONCLUSIONS

A series of PMSQ antireflection coatings were prepared and characterized. The molecular structure and molecular weight may be controlled by grafting different amounts of tetraethoxysilane (TEOS) and 1H,1H,2H,2H-perfluorooctyltriethoxysilane (FTES) to the PMSQ. Compared with pure PMSQ, the minimum reflectivity was reduced dramatically from 3.9 to 0.9% by coating with a single layer and phase segregation. The refractive index at 550 nm was lowered from 1.51 to 1.42 by grafting with FTES and the ensuing molecular rearrangement. Results of EDX and water-contact angle for the PMSQ film provided evidence of phase segregation. The concentration of silicon atoms decreased to 3%, while that of fluorine atoms increased to 22%, and the

water-contact angle increased to 108°, when the weight ratio of MTMS:TEOS:FTES was 1:0.5:1. The advancing water-contact angle and water-contact-angle hysteresis indicated that the surface of the PMSQ film was highly uniform.

#### AUTHOR INFORMATION

##### Corresponding Author

\*E-mail: ccma@che.nthu.edu.tw; Tel: +886-3-5713058.

#### REFERENCES

- (1) Lee, Y. J.; Ruby, D. S.; Peters, D. W.; McKenzie, B. B.; Hsu, J. W. P. *Nano Lett.* **2008**, *8*, 1501–1505.
- (2) Tang, Y. B.; Chen, Z. H.; Song, H. S.; Lee, C. S.; Cong, H. T.; Cheng, H. M.; Zhang, W. J.; Bello, I.; Lee, S. T. *Nano Lett.* **2008**, *8*, 4191–4195.
- (3) Ho, P. K. H.; Thomas, D. S.; Friend, R. H.; Tessler, N. *Science* **1999**, *285*, 233–236.
- (4) Zhang, X. T.; Sato, O.; Taguchi, M.; Einaga, Y.; Murakami, T.; Fujishima, A. *Chem. Mater.* **2005**, *17*, 696–700.
- (5) Ha, J. W.; Park, I. J.; Lee, S. B. *Macromolecules* **2008**, *41*, 8800–8806.
- (6) Hidalgo, M.; Martín, F.; Laserna, J. J. *Anal. Chem.* **1996**, *68*, 1095–1100.
- (7) Walheim, S.; Schäffer, E.; Mlynek, J.; Steiner, U. *Science* **1999**, *283*, 520–522.
- (8) Joo, W.; Park, M. S.; Kim, J. K. *Langmuir* **2006**, *22*, 7960–7963.
- (9) Park, M. S.; Kim, J. K. *Langmuir* **2005**, *21*, 11404–11408.
- (10) Zhang, L. B.; Li, Y.; Sun, J. Q.; Shen, J. C. *Langmuir* **2008**, *24*, 10851–10857.
- (11) Seok, S. I.; Ahn, C. H.; Jin, M. Y. *Mater. Chem. Phys.* **2004**, *84*, 259–262.
- (12) Fu, B. X.; Lee, A.; Haddad, T. S. *Macromolecules* **2004**, *37*, 5211–5218.
- (13) Cardoen, G.; Coughlin, E. B. *Macromolecules* **2004**, *37*, 5123–5126.
- (14) Baney, R. H.; Itoh, M.; Sakakibara, A.; Suzuki, T. *Chem. Rev.* **1995**, *95*, 1409–1430.
- (15) Ohno, K.; Sugiyama, S.; Koh, K.; Tsujii, Y.; Fukuda, T.; Yamahiro, M.; Oikawa, H.; Yamamoto, Y.; Ootake, N.; Watanabe, K. *Macromolecules* **2004**, *37*, 8517–8522.
- (16) Xu, J.; Shi, W. *Polymer* **2006**, *47*, 5161–5173.
- (17) Liu, H.; Xu, J.; Li, Y.; Li, B.; Ma, J.; Zhang, X. *Macromol. Rapid Commun.* **2006**, *27*, 1603–1607.
- (18) Ciolacu, F. C. L.; Choudhury, N. R.; Dutta, N.; Kosior, E. *Macromolecules* **2007**, *40*, 265–272.
- (19) Krishnan, P. S. G.; He, C. *Macromol. Chem. Phys.* **2003**, *204*, 531–539.
- (20) Zhu, B.; Katsoulis, D. E.; Keryk, J. R.; McGarry, F. J. *Polymer* **2006**, *41*, 7559–7573.
- (21) Masuda, T.; Yamamoto, S.; Moriya, O.; Kashio, M.; Sugizaki, T. *Polym. J.* **2008**, *40*, 126–136.
- (22) Sugizaki, T.; Kashio, M.; Kimura, A.; Yamamoto, S.; Moriya, O. *J. Polym. Sci., Part A: Polym. Chem.* **2004**, *42*, 4212–4221.
- (23) Schubert, M. F.; Mont, F. W.; Chhajed, S.; Poxson, D. J.; Kim, J. K.; Schubert, E. F. *Opt. Express* **2008**, *16*, 5290–5298.
- (24) Woo, S. H.; Park, Y. J.; Chang, D. H.; Sobahan, K. M. A.; Hwangbo, C. K. *J. Korean Phys. Soc.* **2007**, *51*, 1501–1506.
- (25) Wang, J.; Wang, L. *J. Fluorine Chem.* **2006**, *127*, 287–290.
- (26) Kim, K. M.; Keum, D. K.; Chujo, Y. *Macromolecules* **2003**, *36*, 867–875.
- (27) Kondo, T.; Yoshi, K.; Horie, K.; Itoh, M. *Macromolecules* **2000**, *33*, 3650–3658.
- (28) Ando, S. *J. Photopolym. Sci. Technol.* **2006**, *19*, 351–360.
- (29) Radcliffe, M. D.; Klun, T. P.; Liu, L. H.; Pokorny, R. J. US Patent 7615283, 2009.